Journal of Petroleum Science and Engineering 120 (2014) 39–51

Contents lists available at ScienceDirect

Journal of Petroleum Science and Engineering

journal homepage: www.elsevier.com/locate/petrol

Studying low-salinity waterflooding recovery effects in sandstone reservoirs

Ahmad Aladasani [a], Baojun Bai [b], Yu-Shu Wu [c], Saeed Salehi [d]

[a] Planning and Support (Heavy Oil), Kuwait Oil Company, Ahmadi, Kuwait
[b] Petroleum Engineering Department, Missouri University of Science and Technology, Rolla, MO., USA
[c] Petroleum Engineering Department, Colorado School of Mines, Golden, CO., USA
[d] Petroleum Engineering Department, University of Louisiana, Lafayette, LA., USA

ARTICLE INFO

Article history:
Received 13 September 2012
Accepted 16 March 2014
Available online 16 April 2014

Keywords:
LSWF
Injected brine salinity
Wettability modification
Injected brine cations
Injected brine anions
Capillary pressure
De-saturation curves

ABSTRACT

Numerous core-flooding experiments have shown that low-salinity water flooding (LSWF) could improve oil recovery in sandstone reservoirs. However, LSWF recovery effects remain highly contentious primarily because of the absence of crucial boundary conditions (boundary conditions are defined throughout the paper as the initial and final, contact angle and interfacial tension values). The objective of this paper is to conduct a parametric study using statistical analysis and simulation to measure the sensitivities of LSWF recovery effects in sandstone reservoirs. The summary of 411 core-flooding experiments discussed in this paper highlights the extent and consistency in reporting boundary conditions, which has two implications for statistical analysis: (1) the statistical correlations of the residual oil saturation to chlorite (0.7891) are strong, whereas the statistical correlations of the residual oil saturation to kaolinite (0.4399) contents, as well as to the wettability index (0.3890), are comparably lower, the majority of dataset entries are missing, and no prediction model can be generated; (2) if a prediction model is generated without clay content values and a wettability index, even though LSWF effects emphasizes wettability modification by virtue of oil aging time and the strong influence of brine cation and divalent ion concentrations on S_{or}, the prediction model's regression curve and confidence level are poor. Reservoir simulations conducted to examine LSWF recovery sensitivities conclude that LSWF recovery effects are governed based on the initial and final wetting states. In all wetting states except for weak water-wet conditions, the increase in oil relative permeability is the underlining recovery effect. In weak water-wet conditions, LSWF incremental recovery is driven by low capillary pressures. In weak oil-wet conditions, the secondary LSWF recovery effect is the change of the non-wetting phase to oil. In all wetting states, an appreciable decrease in interfacial tension (IFT) is realized at the breakthrough recovery. The decrease in IFT is the primary recovery effect in strong water-wet conditions.

1. Introduction

Numerous core-flooding experiments have shown that low-salinity water flooding (LSWF) could improve oil recovery in sandstone reservoirs. Bernard's work in 1967 served as the impetus behind LSWF core-flooding experiments and perhaps low saline solution flooding in other water-based enhanced oil recovery (EOR) methods for the following reasons: (1) core-flooding experiments were conducted on outcrop Berea and Wyoming cores; (2) the results indicated that LSWF improves oil recovery at both the secondary and tertiary stages; (3) residual oil saturation decreased notably when the NaCl weight percentage was reduced from 1% to 0.1%; (4) salinity was advocated as a variable that impacts the efficiency of waterfloods; (5) although the study falls short in detailing oil desorption from the reservoir rock and favorable wettability modifications, the study does attribute incremental recovery from LSWF to fine particle dispersion. Research involving other water-based EOR methods, such as polymer flooding (Paul and Froning, 1973), showed that low-salinity solutions improved the efficiency of polymer drive oil displacement. In addition, several miceller and surfactant flooding field trials have concluded that low-salinity flooding solutions and low divalent ion concentrations can augment oil production (BP, 1979).

The second milestone in the development of LSWF came 30 yrs later when Tang and Morrow (1997) associated LSWF incremental recovery with favorable wettability modification and, 2 yrs later, presented the first LSWF recovery mechanism (Tang and Morrow, 1999a, 1999b). Despite the significance of their contribution,

http://dx.doi.org/10.1016/j.petrol.2014.03.008
0920-4105/

Nomenclature

IFT	interfacial tension
B_w	water formation factor
σ	interfacial tension
B_β	phase β formation factor
S_g	gas saturation
B_w^o	water formation factor at P_b^o
S_o	oil saturation
C_w	water phase compressibility
S_w	water saturation
μ	viscosity
S_{gr}	residual gas saturation
μ_β	phase B viscosity
S_{or}	residual oil saturation
μ_o	oil viscosity
S_{wc}	critical water saturation
μ_w	water viscosity
S_{org}	residual gas oil saturation
M	mobility ratio
S_{gc}	critical gas saturation
λ	mobility ratio
S_{oi}	initial oil saturation
γ	transmissivity
k	permeability
ψ	potential
$k_{r\beta}$	phase β relative permeability
ppm	parts per million
k_{rg}	gas relative permeability
PV	pore volume
k_{ro}	oil relative permeability
g	gas
k_{rw}	water relative permeability
w	water
k_{ro}^{*wo}	oil relative permeability at critical water saturation
o	oil
k_{ro}^{wo}	oil relative permeability in 2-phase oil–water system
ϕ	porosity
k_{ro}^{og}	oil relative permeability in 2-phase oil–gas system
X_c	mass fraction of salt component in the water phase
P_g	gas capillary pressure
X_w	mass fraction of water component in the water phase
P_o	oil capillary pressure
ρ	density
P_w	water capillary pressure
ρ_R	rock grain density
P_β	phase capillary pressure
∇	flux
P_{cgo}	oil gas capillary pressure
ν	Darcy velocity
P_{cow}	water oil capillary pressure
q	flowrate
P_g	bubble point pressure
K_d	salt distribution coefficient between water phase and reservoir rock
P_b^o	initial bubble point pressure
D_m	molecular diffusion coefficient
θ	theta (contact angle)
τ	formation tortuosity
B_g	gas formation factor
P	pressure
B_o	oil formation factor
g	gravity constant
B_w	water formation factor
d	surface depth
B_β	phase β formation factor
B_w^o	water formation factor at P_b^o
Φ	potential
C_w	water phase compressibility
STC	standard tank condition
B_w	water formation factor
R_s	solution gas–oil ratio
B_β	phase β formation factor

rather than attention being drawn to the importance of identifying all boundary conditions in core-flooding experiments, the scientific community turned its focus on identifying LSWF recovery mechanisms and effects. Without knowing critical boundary conditions, several theories were presented, all of which, as expected, were difficult to prove.

The first recovery mechanism suggested for LSWF was the partial stripping of mix-water fines, illustrated in Fig. 1 (Tang and Morrow, 1999a, 1999b), which was questioned in experiments conducted by Zhang et al. (2007) that showed no evidence of clay content in the production stream or the oil/brine interface. The sandstone reservoir is assumed to have a negative charge. The fines comprise of species with dual polarities. During high salinity waterflooding the ionic environment is charged and the fines are adsorbed onto the matrix (the attractive force dominants) thus fines remain adsorbed and do not migrate. By contrast in case the formation water ionic environment is weakened (low-salinity waterflooding) the fines are desorbed from the matrix (repulsive forces dominant).

The second recovery effect suggested for LSWF was the reduction in interfacial tension (IFT) due to an increase in pH values (McGuire et al., 2005), which similarly was questioned in experiments conducted by Lager et al. (2006) showing that LSWF incremental recovery in brine had a pH of less than 7.

The second recovery mechanism suggested for LSWF was based on the concept that multivalent cations bridge the negatively charged oil to the clay minerals (Anderson, 1987; Fairchild et al., 1988; Israelachvili, 1991; Buckley et al., 1989; Liu et al., 2005). In the context of LSWF, Lager et al. (2007) suggested multi-component ionic exchange (MIE), illustrated in Fig. 2. Similar to the partial stripping of mix-water fines the sandstone reservoir is assumed to have a negative charge. As the formation of water is de-ionized (LSWF) the double layer expands due to the weakening attractive force (reduction in cation concentrations). Oil gradually desorbs from the matrix as the repulsive forces become more dominant. MIE resulted in oil desorption when low electrolyte water was used for water flooding, especially Mg^{2+} exchange, which was confirmed by measuring the magnesium content in the produced water (Lager et al., 2007; Alotaibi et al., 2010). This result also was supported by Lee et al. (2010). However, Austad et al. (2010) suggested that polar oil components also can adsorb onto clay minerals without bridging divalent cations, and a reduction in magnesium content can be caused by precipitation, such as $Mg(OH)_2$, especially at increased pH levels during LSWF.

Furthermore, Ligthelm et al. (2009) also suggested that cation striping is not an essential factor in wettability modification. The third LSWF recovery mechanism suggested a relationship between the mineral content kaolinite in clays and the LSWF incremental recovery (Seccombe et al., 2008). However, Cissokho's et al. (2009) experimental findings concluded substantial LSWF incremental recovery in kaolinite-free cores. More than likely, LSWF can create multiple favorable recovery conditions (Austad et al., 2010;

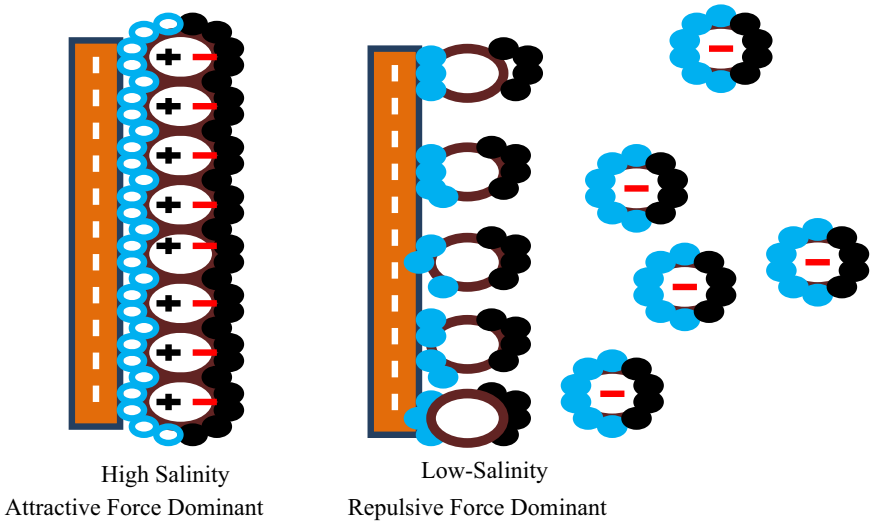

Fig. 1. Partial stripping of mixed-water fines.

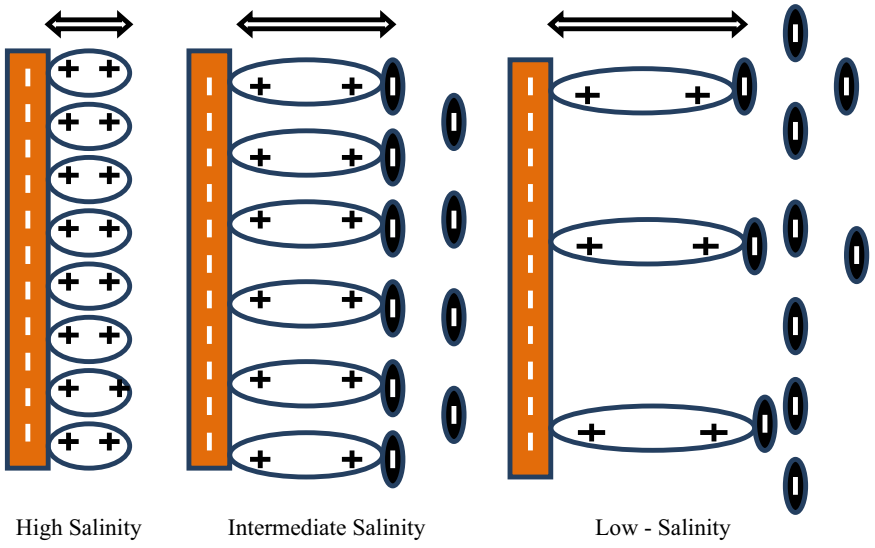

Fig. 2. Multi-ionic exchange in sandstone reservoirs.

Lager et al., 2008a,b) that are variably present; this would explain (a) the varying recovery rates, and (b) the varying reductions in ionic strengths required for LSWF, especially when the heterogeneity of reservoir fluids and rock properties is considered. The work of the aforementioned researchers reiterates the importance of measuring critical boundary conditions in core-flooding experiments.

The third milestone in the LSWF development was the occurrence of field trials and field-scale applications. The first LSWF field trials were conducted by the Kuwait Oil Company (KOC); log-inject-log tests showed a 25 – 50% decrease in residual oil saturation (Webb et al., 2004). The second field trial consisted of single-well chemical tracer tests, which indicated incremental recovery rates from 8% to 19% for four different wells (McGuire et al., 2005). The well with the lowest incremental recovery was flooded with comparably higher salinity, 7000 ppm, than other wells. This observation also has been reported by Zhang et al. (2007), who observed no incremental recovery for cores flooded with a salinity of 8000 ppm. The incremental recovery rates of the remaining three wells ranged from 15% to 19% (McGuire et al., 2005). Published oil production figures for a pilot well (Seccombe et al., 2010) suggest a 10% incremental recovery from June 2008 through April 2009. The salinity was reduced from approximately 27,500 ppm to approximately 13,000 ppm. The oil production rate does not tend to increase with a reduction in water salinity; however, water production figures indicate a clear decrease after the start of LSWF.

A field-wide scale application of LSWF as a secondary recovery method was inadvertently implemented in Syria because the only available source of water was river water (1991–2004). After injecting 0.6 PV of low-salinity water in 2004, produced water was injected thereafter. As of 2009, 0.6 PV of produced water had been injected. The study concluded that wettability alteration resulted in LSWF incremental recovery of 10–15% (Vledder et al., 2010).

The fourth LSWF milestone was reservoir simulation. Jerauld et al. (2006) and Wu and Bai (2009) modeled LSWF as a secondary and tertiary recovery process in a one-dimensional model. The model used by Jerauld et al. (2006) incorporated salinity-dependent fluid relative permeability and capillary pressure functions. Wu and

Bai (2009) model used salinity-dependent oil relative permeability and capillary pressure functions, and a dual-porosity model was presented. Both the models presented for LSWF reservoir simulation consider a linear relationship between the salinity and the fluid residual saturations.

The fifth milestone in the development of LSWF was the measurement of contact angles (Ashraf et al., 2010) and IFT before and/or after core-flooding experiments in carbonate reservoirs (Yousef et al., 2010). The latter work made it possible to generate correlations for residual oil saturation, contact angle and IFT as a function of salinity (Aladasani and Bai, 2012), thus improving the accuracy of LSWF reservoir simulation and making it possible to conduct reservoir simulation parametric studies that measure the sensitivities of LSWF recovery effects.

The objective of this paper is to conduct a parametric study to measure the sensitivities of LSWF recovery effects in sandstone reservoirs. The first approach is based on the statistical analysis of 411 sandstone core-flooding experiments. The second approach is based on an LSWF recovery sensitivity analysis carried out by a compositional simulator.

Table 1
Summary of core-flooding experiments.

Paper reference	Number of plugs/ cores	Secondary recovery runs	Tertiary recovery runs	Irreducible water saturation	Formation brine ions	Injection fluid cationic	Viscosity	Aging temperature	Aging time	Test temperature	IAH	IFT	Clay (wt%)	Calcite (wt%)	Kaolinite (wt%)
Yildiz et al. (1999)	13	13	0	√	√	√	√	√	√	√	X	X	X	X	X
Austad et al. (2010)	1	1	1	√	√	√	√	√	√	√	X	X	√	X	X
Tang and Morrow (1997)	21	21	3	√	√	√	√	√	√	√	X	√*	X	X	X
Boussour et al. (2009)	1	1	0	√	√	√	√	√	√	√	X	X	√	√	√
Agbalaka et al. (2008)	16	16	80	√	√	√	√	√	√	√	X	X	X	X	X
Ashraf et al. (2010)	12	12	0	√	√	√	√	√	√	√	√	X	X	X	X
Robertson (2010)	23	23	0	√	√	√	√	√	X	√	X	X	X	X	X
Bernard (1967)	15	14	20	√	√	√	X	X	X	X	X	X	X	X	X
Zhang and Morrow (2006)	34	34	2	√	√	√	√	√	√	√	X	X	X	X	X
Zhang et al. (2007)	2	11	10	√	√	√	√	√	√	√	X	X	X	X	X
Ligthelm et al. (2009)	1	2	2	X	√	√	√	√	X	√	X	X	X	X	X
Pu et al. (2010)	9	9	9	√	√	√	√	√	√	√	X	X	X	X	X
Hadia et al. (2011)	14	14	28	√	√	√	√	√	√	√	√*	X	√*	√*	√*
Gamage and Thyne (2011)	12	12	12	√	√	√	√	√	√	√	X	X	X	X	X
Nasralla et al. (2011a)	8	8	0	√	√	√	√	√	X	√	X	X	X	X	X
Thyne and Gamage (2011)	4	4	2	√	√	√	√	√	X	√	X	X	√	X	X
Nasralla et al. (2011b)	8	8	6	√	√	√	√	√	X	√	X	X	√	√	√
Rivet et al. (2010)	17	8	11	X	√	√	√	√	√	√	X	X	√*	X	X
Sharma and Filoco (2000)	X	12	2	X	√	√	√	X	X	X	X	X	X	X	X
Total	**211**	**214**	**188**	**374**	**411**	**411**	**365**	**397**	**308**	**397**	**78**	**22**	**66**	**48**	**48**

* indicates that only an initial measurement was recorded.

2. Methodology

The methodology consists of two main sections, the first of which pertains to the use of statistical analysis tools to evaluate LSWF sensitivities in core-flooding experiments, and the second of which describes the use of a compositional simulator to examine LSWF recovery effects.

A sandstone core-flooding experiment database was built based on the published journal and conference papers. The database consists of 411 LSWF experiments, of which 223 are secondary mode recovery and 188 are tertiary mode recovery. In addition, reported fluid and core properties were included, such as irreducible water saturation, wettability, IFT, clay content, aging and test temperatures, as presented in Table 1, which appears at the end of this paper. Statistical representation of the core-flooding database will be provided on http://www.eorcriteria.com.

The summary of core-flooding experiments highlights the extent and consistency in reporting boundary conditions. It is evident that capillary pressure variables, such as wettability and IFT, are reported infrequently, having a total of only 78 and 22 entries, respectively, out of 411 in the core-flooding database.

Similarly, clay content and the weight percentages of chlorite and kaolinite are reported to be 66, 48 and 48 times out of 411 in the database. The statistical analysis conducted for the low-salinity core-flooding database comprises two stages. In the first stage, correlations are evaluated for the reported variables in the core-flooding experiments. Correlation measurements are required in order to screen sensitivities of various core-flooding variables versus the intended outcome, "residual oil saturation." Evaluating key variables in LSWF is critical in generating a prediction model because strong correlations will improve the accuracy of the multivariable regression curve. The restricted maximum likelihood (REML) method was used to examine the relationships between the variables in the core-flooding experiments. The entire database, consisting of 411 low-salinity core-flooding experiments, is fed into the JMP statistical software, and one-to-one correlations are generated, as presented in Fig. 3, which appears at the end of this paper. Fig. 3 is a matrix representation of the core-flooding experiment variables and their correlations to each other. As an example the permeability has 0.2605, 0.0716 and 0.0617 correlations with the initial water saturation (Swi), cations (Swi) and injected brine cations, respectively. The correlation values can be read along either axis:

$$R^2 = \frac{\sum square\ (model)}{\sum square/degrees\ of\ freedom} \tag{1}$$

The results in Fig. 3 indicate strong correlations between the S_{or} and chlorite (0.7891) and kaolinite (0.4399) contents, in addition to the wettability index (0.3890); however, none of these strong correlations can be used because the majority of LSWF core-flooding experiments fail to report clay content or wettability. Without strong correlations, the prediction model will have poor accuracy and confidence limits, as demonstrated by generating a prediction model without the previously mentioned variables that affect capillary conditions, as shown in Fig. 4.

The prediction plot in Fig. 4 demonstrates the accuracy of the multivariable regression curve based on the distribution of the dataset (distance away from the solid line). The prediction profiler shows the impact of the experimental variables selected on the residual oil saturation (S_{or}) along with the corresponding confidence level for each experimental variable. As an example, brine cations at Swi and aging time (days) have a strong impact on S_{or}. The aging time (days) confidence level is the best amongst the selected experimental variables (since the tolerance is low over a

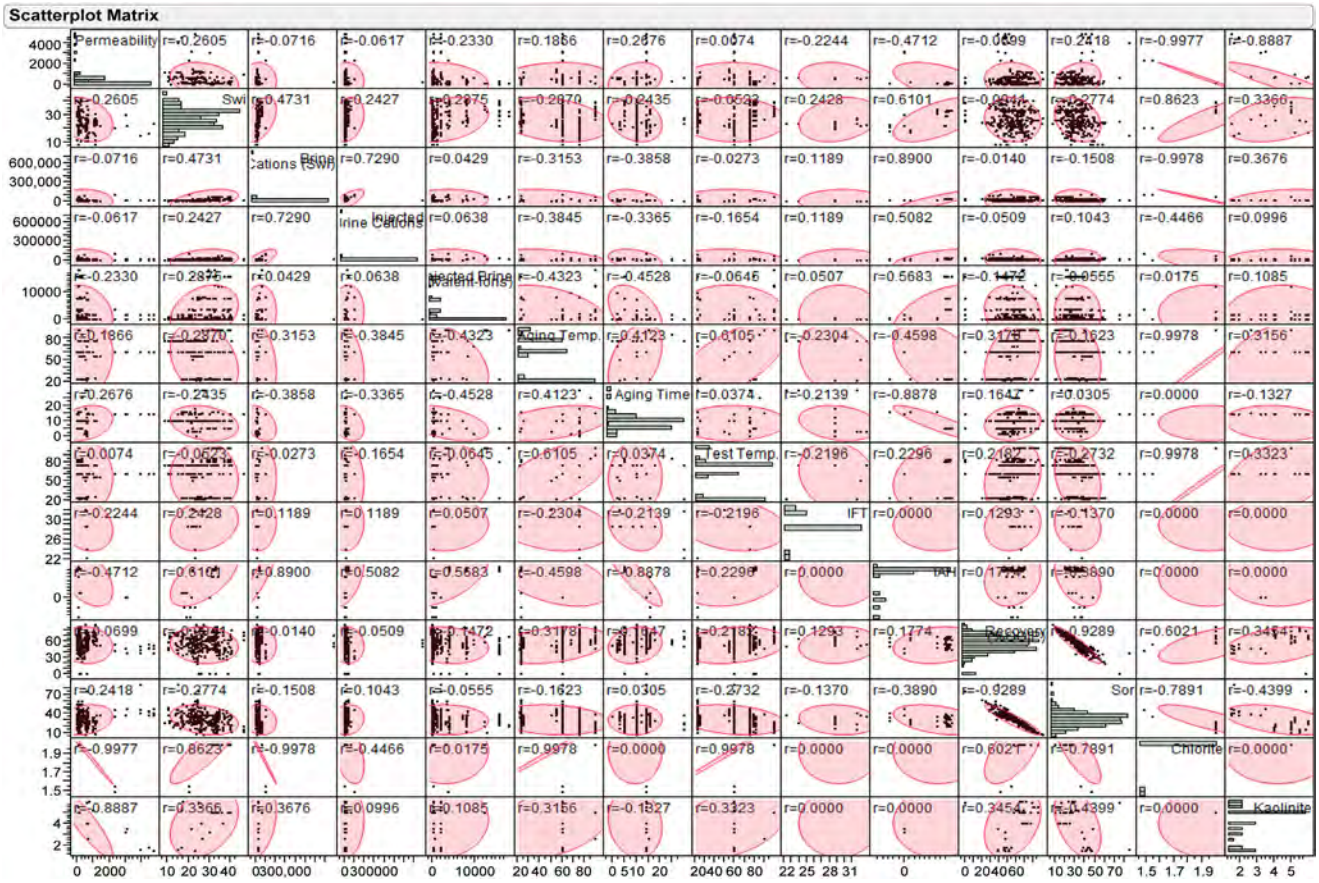

Fig. 3. Core-flooding experiment correlations.

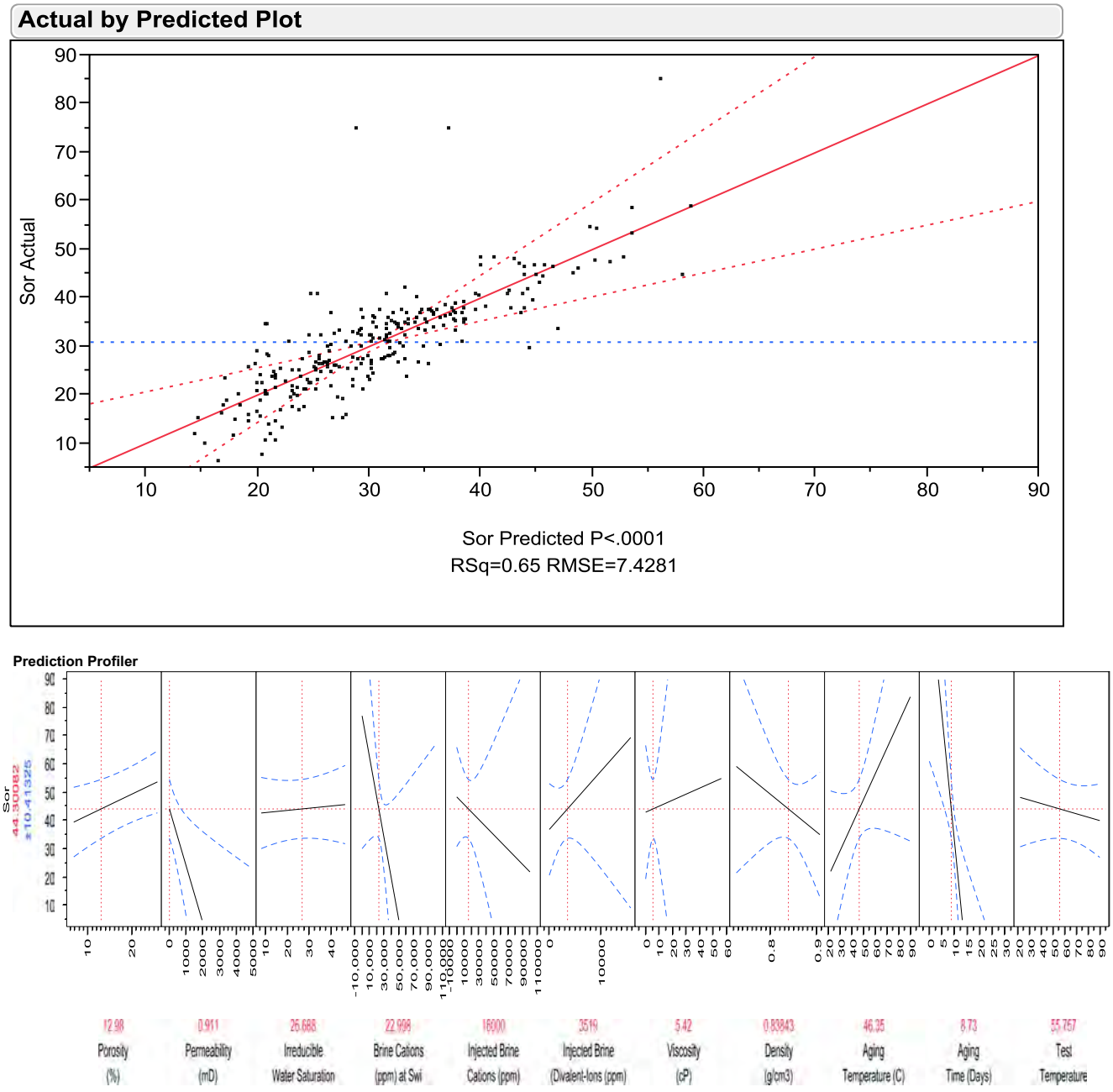

Fig. 4. Residual oil saturation prediction model (excluding wettability & clay content).

wide range of days). The multivariable regression curve and the confidence level both exhibit poor accuracy, and as a result, the impact of each core-flooding variable on S_{or} cannot be examined.

However, the results in Fig. 4 indicate, in order, that the oil aging time, brine cation concentration at S_{wi} and divalent ion concentration in the injected brine strongly influence S_{or}, which emphasizes the possible role of wettability modification in LSWF.

Simulating LSWF in sandstone reservoirs involves the following development stages. (1) Phase behavior in porous media. (2) Handling immobile water zone. (3) Relative permeability and capillary pressure functions for LSWF in sandstone reservoirs. And (4) validating the model analytically.

2.1. Physical Processes and Constitutive Equations

Reservoir simulation is based on the law of conservation, constitutive equations and equations of state. The reservoir is considered a controlled volume containing three phases and various mass components. The saturation occupied by each phase in the porous media is a representation of the fractional phase volume. Therefore, using material balance equations, the mass component in the gas, oil and water phases can be derived. Constitutive equations are needed to determine the phase pressure and relative permeability, which is achieved by relating the phase, saturations and mass components. As a result, it is possible to derive capillary pressure and relative permeability expressions as a function of phase saturations and mass component fractions.

In LSWF, salt is considered a mass component in the water phase, which is expressed by the product of the reservoir's porosity, water saturation, water density and salt mass component; as such, salt is transported by advection. Additionally, because the salt mass component in the water phase is transported by diffusion and in sandstone reservoirs cations are prone to adsorption on the reservoir rock, an expression is required to

differentiate the fate of adsorbed salt and salt transported by diffusion (based on Eq. (2)). A tortuosity term is added to the equation to account for increases in the distance that molecules must travel in a porous media.

Constitutive equations are needed to determine the phase pressures, saturations and phase relative permeabilities; this is achieved by relating the phase, saturations and mass components. The sum of saturations of hydrocarbon phases equals unity, as does the sum of mass components in any phase:

$$X_w + X_c = 1 \tag{2}$$

The phase pressure is, by definition, the difference between the non-wetting phase and the wetting phase. The non-wetting phase always has a higher pressure than the wetting phase, and gas is always the non-wetting phase in hydrocarbon reservoir rocks (Satter et al., 2008). Similarly, the three-phase capillary pressure between the water and the oil interface is shown in Eq. (3). The water phase consists of two mass components, so both mass fractions are a function of water–oil capillary pressure. This relationship makes it possible to consider the effects of LSWF on capillary pressure. In addition, capillary pressure correlations, such as those provided in Parker et al. (1987), do not consider IFT parameters in the capillary function. Therefore, a J-function can be used to relate changes in both IFT and the contact angle as a result of LSWF:

$$P_o - P_w = P_{cow}(S_w,\ S_o,\ X_c) \tag{3}$$

$$P_{cow} = \sigma(X)\ \cos\ \theta(X) P^0_{cow}(S_w, S_o) \tag{4}$$

By definition, the relative permeabilities are functions of the saturations occupying the porous media and also should include the phase mass components, as shown in Eq. (5). The Stone correlation, method II (Aziz and Settari, 1979), can be used if no three-phase relative permeability data is available. The Stone correlation provides three-phase relative permeability data based on two sets of two-phase flow relative permeabilities:

$$k_{rw} = k_{rw}(S_w, X_c) \tag{5}$$

The equation of state describes phase density as a function of temperature and pressure; this is represented by the phase formation factor. The water phase density is a function of temperature, pressure and the salt mass component, as shown in Eq. (6). Gas and oil viscosities are treated as functions of phase pressure only, and the water phase viscosity is a function of the salt mass component, as shown in Eqs. (8) and (9). The water phase viscosity is treated as a function of the salt mass component to evaluate the mobility ratio during LSWF:

$$\rho_w = \frac{[\rho_w(X_c)]_{STC}}{B_w} \tag{6}$$

where

$$B_w = \frac{B^o_w}{1 + C_w(P_w - P^o_b)} \tag{7}$$

$$\mu_\beta = \mu_\beta(P_\beta) \tag{8}$$

$$\mu_w = \mu_w(X_c) \tag{9}$$

2.2. Handling Immobile Water Zones

Immobile or residual water zones of in situ brine within porous pores can be handled as separate domains containing immobile water only, such as “dead” pores, acting as additional continuums with zero permeability. The salt within the immobile zones will interact with mobile water zones by diffusion only. This diffusion process is described by the same governing equations and numerical formulations discussed above as a special no-flow case.

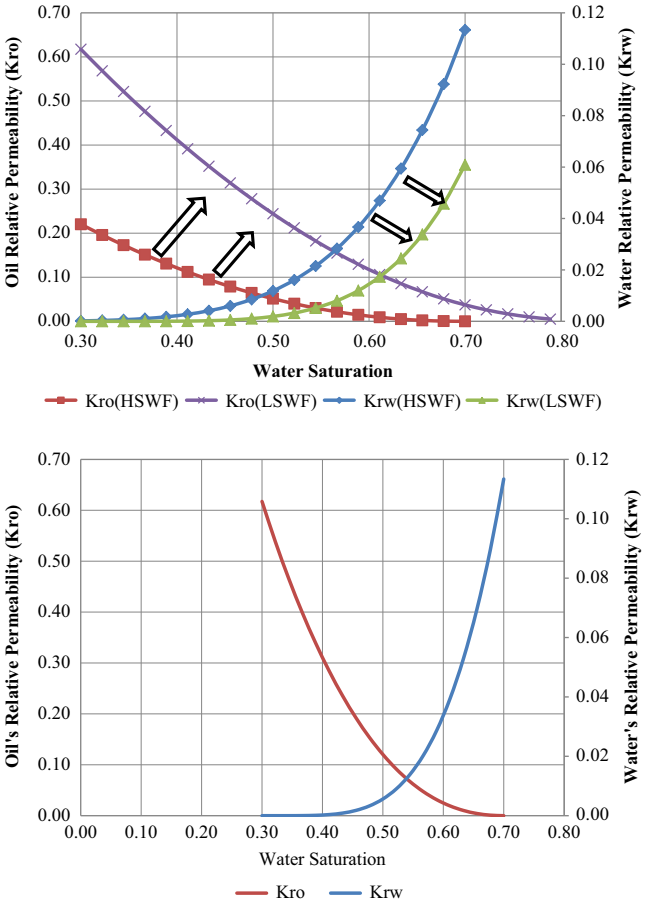

Fig. 5. (a) Fluid relative permeability curves. (b) High to low salinity waterflooding relative permeability curves.

2.3. Relative Permeability and Capillary Pressure Functions

The model considered two relative permeability and capillary pressure formulations, the first being a linear relationship proposed by Jerauld et al. (2006), and the second based on correlations from core-flooding experiments provided by Tang and Morrow (1997) (Eq. (14)). Evidently, core-flooding experiments reveal a near linear relation between salinity and residual oil saturation. Published IOR effects for LSWF emphasize the decrease residual oil saturation. Therefore, relative permeability functions are modified accordingly to include the effects of salinity.

The Brooks–Corey function (Honarpour et al., 1986) is used with the following modifications: (1) decrease in relative permeability to water phase as salinity decreases, and (2) increase in relative permeability of oil phase as salinity decreases. The Brooks–Corey exponential index φ (Corey, 1954) is adopted, and two normalized fluid saturations are described in Eqs. (12) and (13). The residual oil saturation is considered as a function of salinity in the aqueous phase and, hence, a function of water's relative permeability. Jerauld et al. (2006) first proposed a linear relationship between the salt mass component and the residual oil saturation and treated salt mass concentration as a function of both oil and water's relative permeability. In this equation, S_{or1} is the maximum residual oil saturation at a high salt mass fraction, X_{c1}, and S_{or2} is the minimum residual oil saturation at a low salt

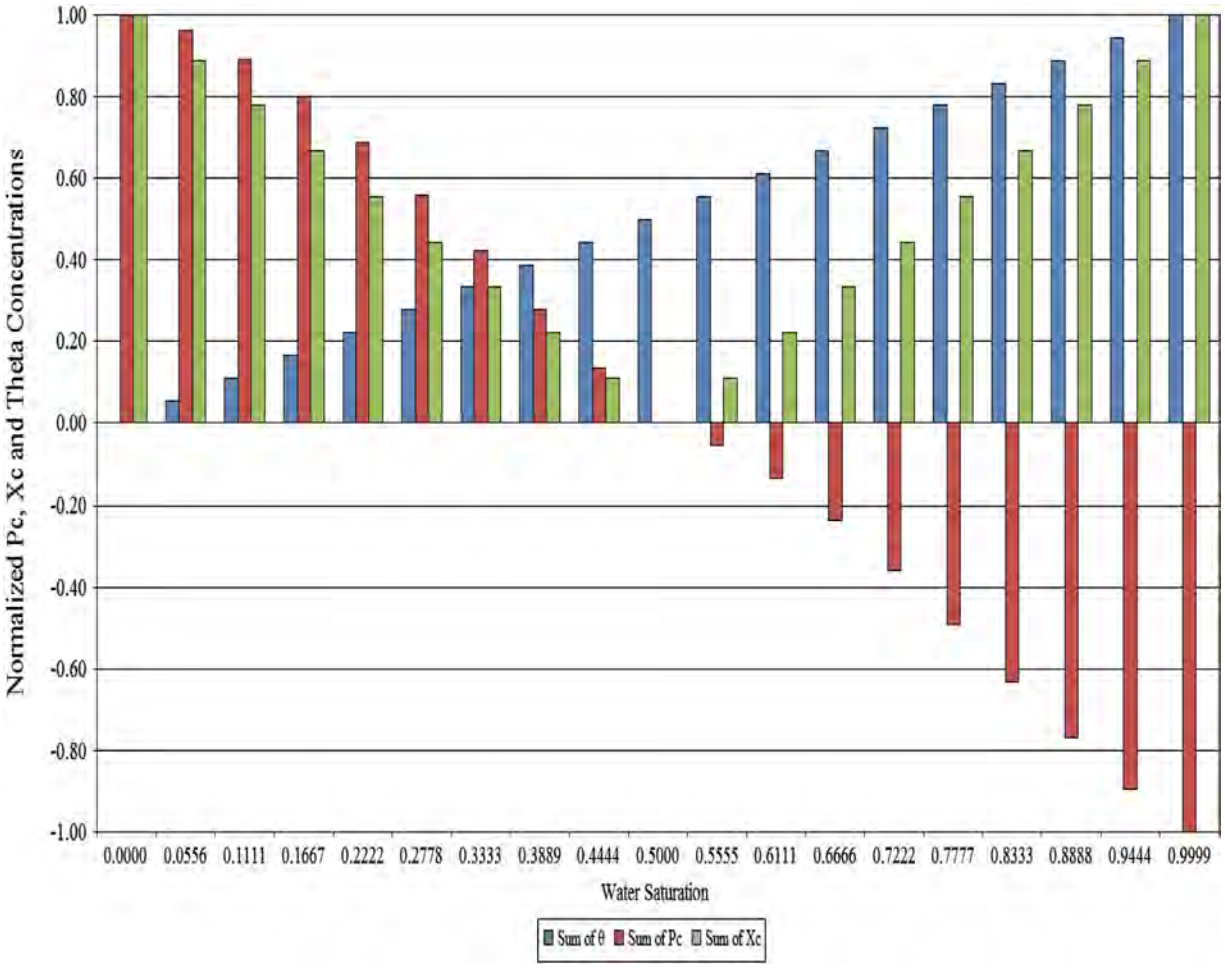

Fig. 6. Capillary pressure curves.

mass fraction, X_{c2}:

$$k_{rw} = (\bar{S}_w)^{2+\varphi}[\bar{S}_w(X_c)] \tag{10}$$

$$k_{ro} = (\bar{S}_o)^2[1-(\bar{S}_w)^{\varphi}] \tag{11}$$

$$\bar{S}_w = \frac{S_w - S_{wr}}{1 - S_{wr}} \tag{12}$$

$$\bar{S}_o = \frac{S_o - S_{or}(X_c)}{1 - S_{wr}} \tag{13}$$

$$S_{or}(X_c) = S_{or1} + \frac{(-0.1083)(X_c)^2 + (1.244)(X_c) + (-4.694e-8)}{(X_c) + 0.1353}(S_{or1} - S_{or2}) \tag{14}$$

Capillary pressure functions are modified to include the effects of salinity. A linear relationship to residual oil saturation is introduced between the salt mass fraction and the contact angle so that a decrease in the salt mass fraction would favorably alter wettability to intermediate wetting conditions, as shown in Eq. (15). In this equation, θ_{or1} is the contact angle at a high salt mass fraction, X_{c1}, and θ_{or2} is the contact angle at a low salt mass fraction, X_{c2}. The capillary pressure function from Van Genuchen (1980) and Parker et al. (1987) is used for the oil–water system, with the addition of the cosine of contact angles of the oil and water phases on the rock's surface to include the effect of low salinity on the contact angle, as shown in Eq. (16), where α_{vG}, γ and β are parameters of the Van Genuchen functions (Van Genuchen, 1980), in which $\gamma = 1 - 1/\beta$ (Wu and Bai, 2009):

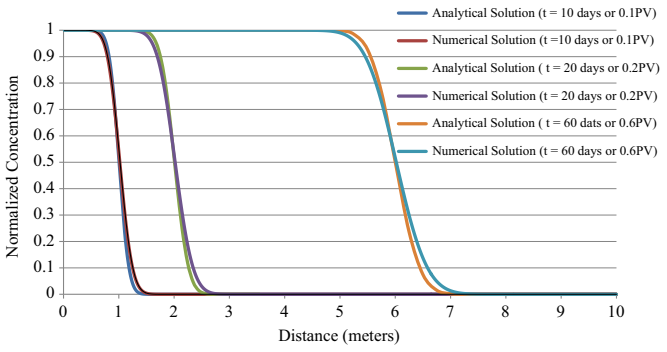

Fig. 7. Analytical versus numerical solution to Problem 1.

$$\theta(X_c) = \theta_{or1} + \frac{X_c - X_{c1}}{X_{c1} - X_{c2}}(\theta_{or1} - \theta_{or2}) \tag{15}$$

$$P_{cow} = \frac{\cos\theta\rho_w}{(\cos\theta\rho_w)^o}\left(\frac{g}{\alpha_{vG}}\right)[(1-S_w)^{-1/\gamma} - 1]^{1/\beta} \tag{16}$$

The fluid relative permeability functions in Eqs. (10) and (11) and the capillary pressure function in Eq. (16) are illustrated in Figs. 5b and 6, respectively. When oil enters the wetting phase, the capillary pressure and salinity magnitudes increase away from intermediate wetting conditions, and the capillary pressure changes to a negative convention, as shown in Fig. 6.

Table 2
Sandstone Core Plug Properties (Taken from Ashraf et al., 2010).

Wettability type	Contact angle (assumed)	Initial IFT (assumed)	Core #	Injection brine (% salinity)	Porosity (ϕ)	Permeability (md)		S_{wi} (% PV)
						Air	Brine (assumed)	
Water-wet (I_{AH}=0.63)	25	30 dynes/cm	A2	100	18.2	82	54	32
			A3	10	18.2	78	51	34
			A4	1	18.0	77	50	31
Neutral wet (I_{AH}=0.12)	70		B2	100	19.3	185	122	17
			B3	10	19.3	178	117	19
			B4	1	19.0	167	110	18
Neutral wet (I_{AH}=−0.27)	117		C2	100	18.0	66	43	18
			C3	10	19.2	86	56	21
			C4	1	19.2	78	51	23
Oil-wet (I_{AH}=−0.57)	141		D2	100	19.1	82	54	19
			D3	10	19.1	78	51	21
			D4	1	19.0	72	47	21

Table 3
Sandstone core-flooding fluid properties (taken from Ashraf et al., 2010).

Water type	**TDS (ppm)**	**Density (kg/m^3)**	**Viscosity (mPa s)**
Connate water	38,522	1031 (assumed)	1.083 (assumed)
Synthetic brine (100%)	24,951	1019	1.052
Synthetic brine (10%)	2495	1001	1.008
Synthetic brine (1%)	249	999	1.010

Table 4
Sandstone Core (A) Case 1 simulation versus core-flooding results.

Core-flooding experiment (taken from Ashraf et al., 2010)				Numerical simulator (no change in capillary pressure)		
Core #	Breakthrough recovery % OOIP	Final recovery %OOIP	S_{or} (% PV)	Contact angle	Breakthrough recovery % OOIP	Final recovery %OOIP
A2	43	49	35		45.0	47.8
A3	50	56	29	25°	50.0	54.7
A4	61	69	21		55.6	65.3

2.4. Model Validation

The compositional simulator ability to model a mass component in the water phase is validated analytically. In Problem 1, we consider the one-dimensional transport of a chemical component in a homogeneous, water-saturated, porous medium that is 10 m long, similar to the one used by Wu et al. (1996). It has a steady-state flow field with a 0.1 m/day velocity. A chemical component is introduced at the inlet (x=0) with a constant concentration, and transport starts at t=0 by advection and diffusion. This problem is solved numerically by specifying both the inlet and outlet boundary elements with constant pressures, which give rise to a steady-state flow field with a 0.1 m/day pore velocity. The constant pressures are determined by specifying the following reservoir properties: a permeability of 0.898×10^{-12} m^2, a viscosity of 0.898×10^{-3} Pa s and a 10-meter long domain with a unit cross-sectional area. The analytical solution to Problem 1 is generated by a computer program based on the analytical solution reached by Javandel et al. (1984).

A comparison of the salt concentrations along the rock column from the numerical and analytical solutions is shown in Fig. 7 for t=10, 20 and 60 days, respectively. The results, shown in Fig. 7, indicate good agreement between the analytical solution and the numerical solution.

Table 5
Sandstone Core (A) Case 2 simulation versus core-flooding results.

Core-flooding experiment (taken from Ashraf et al., 2010)				Numerical simulator (capillary pressure zero)		
Core #	Breakthrough recovery % OOIP at PV1	Final recovery % OOIP at PV6	S_{or} (% PV)	Contact angle	Breakthrough recovery % OOIP	Final recovery %OOIP
A2	43	49	35		45.2	48
A3	50	56	29	25°	50.7	55.2
A4	61	69	21		58.8	67.7

Table 6
Sandstone Core (A) Case 3 simulation versus core-flooding results.

Core-flooding experiment (taken from Ashraf et al., 2010)			Numerical simulator (no change in capillary pressure)		
Core #	Breakthrough recovery %OOIP	Final recovery % OOIP	Contact angle	Breakthrough recovery %OOIP	Final recovery % OOIP
A2	43	49		45.0	47.8
A3	50	56	25°	50.3	54.7
A4	61	69		60.2	66.8

Table 7
Sandstone Core (A) Case 4 simulation versus core-flooding results.

Core-flooding experiment (Taken from Ashraf et al., 2010)			Numerical simulator (no capillary pressure)		
Core #	Breakthrough recovery %OOIP	Final recovery % OOIP	Contact angle	Breakthrough recovery %OOIP	Final recovery % OOIP
A2	43	49		45.1	48.0
A3	50	56	25°	50.6	55.2
A4	61	69		60.7	67.7

3. Application and results

This section is designed to examine the accuracy of the model's formation and numerical implementation in simulating one-dimensional immiscible displacement, in which oil in a one-dimensional linear rock column is displaced by water. The reservoir rock's wettability and injected water salinity are modified to examine the impact on oil recovery. Published core-flooding experiments will

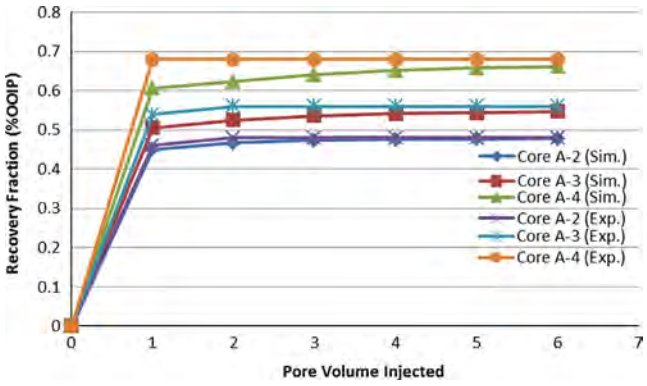

Fig. 8. Oil recovery curves for Table 4 sandstone Core (A) Case 4.

be compared with simulation results. The flow domain in Problem 2 consists of 12 one-dimensional, horizontal, homogeneous, and isotropic porous media 5 cm long with a diameter of 3.8 cm. The one-dimensional radial domain is represented by 100 uniform grid blocks, each with a cross-sectional area of 11.34 cm^2 and a uniform mesh spacing ($\Delta x = 0.05$ cm). The numerical model is solved fully implicitly with a maximum time limitation set to 1 s. The problem sets consider four different wetting conditions and three cores for each wetting condition, with a slight an increase in permeability for Cores B2–B4, as shown in Table 2. The brine permeability was assumed to be two-thirds of the air permeability. The system initially is saturated with oil and water, the latter of which is at its irreducible saturation. Water with three different salinities, as shown in Table 3, is injected as a displacing fluid at the inlet to drive oil out of the porous medium domain at a constant rate of 6 ml/min (0.5 cm^3 per minute). The recovery rates for water flooding with the three different salinities are compared for each crude type (wettability).

In Case 1, water-wet cores, Cores A2–A4, as described in Table 2, are examined, and four sets of simulation runs are conducted. In the first set of simulations, it is assumed that water's relative permeability remains constant. The intent is to examine how well the simulation results match those of the core-flooding experiments when the salinity concentration is considered solely as a function of oil relative permeability (Wu and Bai, 2009); the results are shown in Table 4. In the second set of simulations, zero capillary pressure conditions are assumed; these results are shown in Table 5. In the third set of simulations, it is assumed that, similar to oil, water relative permeability is also a function of salinity concentration; the results are shown in Table 6.

The intent is to validate the mathematical model formulation related to relative permeability curves presented by Jerauld et al. (2006). The fourth set of simulations is similar to the third set; however, the capillary pressure is considered zero, and the results are shown in Table 7.

The recovery results in Table 4 indicate some variances between the simulation and experimental results. These variances are proportional to salinity, as is evident for Core A4, in which the variances for breakthrough and final recovery are 4.4% OOIP and 3.7% OOIP, compared to Core A2, in which the variances are 2% OOIP and 1.2% OOIP, respectively. In addition, the core-flooding experiment's final recovery rates are all higher than the simulation results. It could be possible that the IFT was assumed too high, or that the irreducible water saturation (S_{wr}) may increase with LSWF. To further evaluate the results in Table 4, a new set of simulation runs (Case 2) is conducted assuming no capillary pressure effects.

The recovery results in Table 5 indicate that the variances decrease when no capillary pressure conditions exist. The variance between the core-flooding experiment and the simulation results for Cores A2, A3 and A4 is 1%, 0.8% and 1.3% OOIP, respectively.

Table 8
Sandstone Core (B) Case 5 simulation versus core-flooding results.

Core-flooding experiment (Taken from Ashraf et al., 2010)			Numerical simulator (no change in capillary pressure)		
Core #	Breakthrough recovery %OOIP	Final recovery % OOIP	Contact angle	Breakthrough recovery %OOIP	Final recovery % OOIP
B2	60	63		57.8	61.2
B3	60	67	70°	58.3	67.1
B4	61	72		58.8	70.6

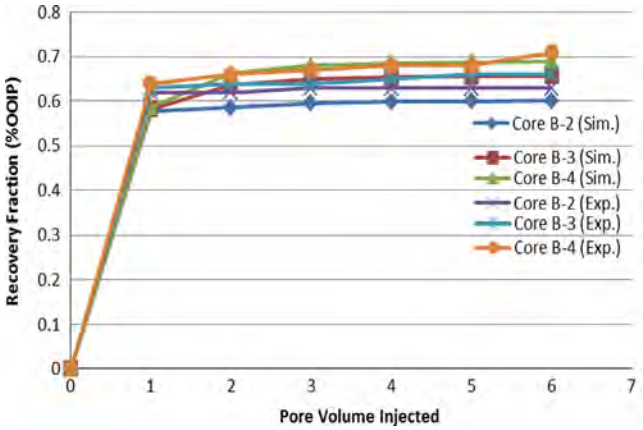

Fig. 9. Oil recovery curves for Table 8 sandstone Core (B) Case 5.

Table 9
Sandstone Core (C) Case 6 simulation versus core-flooding results

Core-flooding experiment (taken from Ashraf et al., 2010)			Numerical simulator (change in contact angle up to 91°)		
Core #	Breakthrough recovery %OOIP	Final recovery % OOIP	Contact angle	Breakthrough recovery %OOIP	Final recovery % OOIP
C2	44	51		42.0	49.2
C3	49	58	117°	43.3	54.6
C4	45	66		46.7	60.1

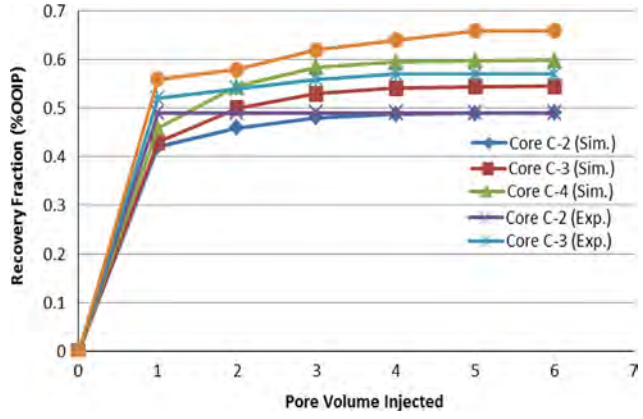

Fig. 10. Oil recovery curves for Table 9 sandstone Core (C) Case 6.

However, the assumption of a zero capillary pressure condition is intended for evaluation only. Another possible explanation is that the irreducible water saturation increases during LSWF. To evaluate this assumption, additional simulations (Case 3) are

Table 10
Sandstone Core (D) Case 7 simulation versus core-flooding results.

Core-flooding experiment (taken from Ashraf et al., 2010)				Numerical simulator (no change in capillary pressure)			
Core #	Breakthrough recovery %OOIP	Final recovery %OOIP	S_{or} (% PV)	Contact angle	Breakthrough recovery %OOIP	Final recovery %OOIP	S_{wr} (% PV) final
D2	46	54	37		50.2	53.4	23
D3	53	56	36	141°	50.4	53.4	22
D4	57	61	30		55.8	60.4	27

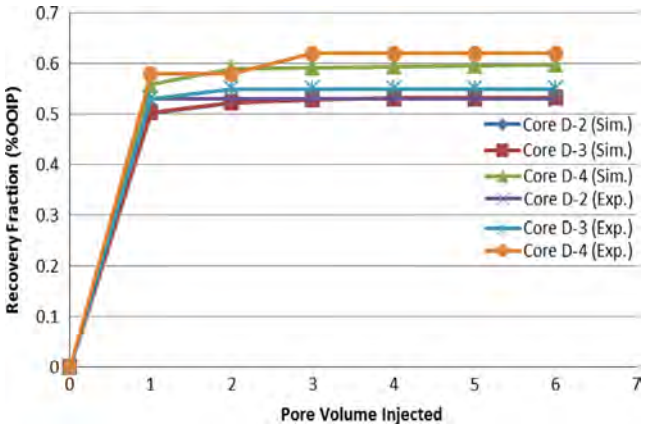

Fig. 11. Oil recovery curves for Table 10 sandstone Core (D) Case 7.

Contact Angle	141° to 117%	117° to 70°	70° to 25°
Experiment	A. -3% B. 2% C. 5%	A. 12% B. 9% C. 6%	A. -14% B. -11% C. -3%
Simulation	A. -4.2% B. 1.2% C. -0.3%	A. 12% B. 12.5 C. 10.5%	A. -13.6% B. -12.8% C. -3.8%

Legend : A – 100% Salinity, B – 10% Salinity, C – 1% Salinity, % = %OOIP

Fig. 12. Variance of recovery fraction (%OOIP) as a function of wettability.

conducted considering a decrease in water relative permeability as the displacing water's salinity is decreased.

The summarized results in Table 6 indicate good agreement between the numerical simulator and the core-flooding experiments and suggest that the irreducible water saturation increases during LSWF. Additional simulations summarized in Table 7 and Fig. 8 (Case 4) are required to examine the impact of capillary pressure on oil recovery versus the fluid's relative permeability. It is assumed that capillary pressure is zero.

The following is suggested for LSWF in strong water-wet reservoirs: (1) the irreducible water saturation increases during LSWF; (2) the underlying recovery effect in LSWF is the increase in oil relative permeability, which accounts for incremental recovery rates up to 19% OOIP; (3) the reduction in capillary pressure accounts for incremental recovery of about 0.9% OOIP.

In Case 5, weak water-wet cores are examined; these consist of Cores B2–B4, as described previously in Table 1. An IFT of 30 dynes/cm and contact angle of 70° are held constant. Table 8 and Fig. 9 show a comparison of oil recovery rates between the core-flooding experiments and the simulation results, indicating very good agreement for both breakthrough and final recovery. The breakthrough recoveries are comparable for all salinities and higher than for the strong water-wet cores. This implies that in weak water-wet systems, LSWF recovery is governed by the low capillary pressure.

In Case 6, weak oil-wet cores are examined; these consist of Cores C2–C4, as described previously in Table 2. An IFT of 30 dynes/cm, an initial contact angle of 117° and a final contact angle of 91° are assumed. Table 9 shows a comparison of oil recovery rates between the core-flooding experiments and the simulation results. The breakthrough recovery and final recovery for both the experimental and simulation results agree well, with the exception of the final recovery in Core #C4. The results in Table 9 and Fig. 10 suggest that in weak oil-wet systems, LSWF recovery is influenced by the increase in oil relative permeability (13.4% OOIP), followed by the decrease in the capillary pressure when oil becomes the non-wetting phase (about 6% OOIP).

In Case 7, Cores D2–D4, the oil-wet cores described previously in Table 2, are examined. An IFT of 30 dynes/cm and a contact angle of 141° are assumed. To establish a baseline, the contact angle and IFT are held constant for all the water-flooded cores in order to examine the influence of relative permeability on recovery.

Table 10 provides a comparison of oil recovery rates between the core-flooding experiments and the numerical simulator. The results in Table 10 and Fig. 11 indicate good agreement for the final recovery between the simulation and the experimental results. It is suggested that in oil-wet systems, the increase in oil relative permeability is the underlying recovery effect. The variance in the breakthrough recovery is subject to the selection of the initial contact angle.

Several points must be considered prior to contrasting numerical simulations with core-flooding experiments. The major challenge is rock homogeneity; once a rock type is declared in a numerical simulator and assigned oil and geological characteristics, those reservoir properties are considered uniformly distributed.

In reality, however, oil saturations are not distributed evenly across the length of the core. Consequently, numerical simulation recovery rates for core-flooding experiments will vary, especially at breakthrough. Therefore, it is imperative to include an adequate number of elements to control the variances in breakthrough and final recovery. The occasional use of air permeability rather than brine permeability also impacts the variances between core-flooding experiments and simulation. Finally, core-flooding experiments should be reported consistently, and boundary conditions should be measured before and after the experiment is executed, especially when the boundary conditions in question are advocated as recovery mechanisms.

4. Analysis

The majority of core-flooding experiment advocate wettability modification as the most likely LSWF recovery mechanism however only a few experiments measure contact angle and IFT and most of the core-flooding experiments start with intermediate wetting conditions. The initial wetting conditions, final wetting conditions and the associated change in wetting conditions are a

result of modifying the injected brine ionic composition. Therefore, in Fig. 12, the variance in oil recovery (fraction of %OOIP) is illustrated as a function of initial and final wetting conditions. Fig. 12 outlines the benefits of LSWF at various wetting states and when LSWF should be seized to avoid unfavorable wettability modification.

5. Conclusion

The summary of 411 core-flooding experiments highlights the extent and consistency in reporting boundary conditions, with the following two implications for statistical analysis: (1) the statistical correlations of the residual oil saturation to chlorite (0.7891) are strong, whereas the statistical correlations of the residual oil saturation to kaolinite (0.4399) contents, as well as to the wettability index (0.3890), are comparably lower, the majority of dataset entries are missing, and no prediction model can be generated; (2) if a prediction model is generated without the clay content and a wettability index, even though LSWF emphasizes wettability modification by virtue of the strong influence on S_{or} of oil aging time, brine cation and divalent ion concentration, the prediction model regression curve and confidence level will be poor.

Reservoir simulations conducted to examine LSWF recovery sensitivities conclude that LSWF recovery effects are governed based on capillary conditions. In all wetting states except for weak water-wet conditions, the increase in oil relative permeability is the underlining recovery effect. In weak water-wet conditions, LSWF incremental recovery is driven by low capillary pressures. In weak oil-wet conditions, the secondary LSWF recovery effect is the change of the non-wetting phase to oil. In all wetting states, an appreciable decrease in interfacial tension (IFT) is realized at the breakthrough recovery. The decrease in IFT is the primary recovery effect in weak water-wet conditions.

References

Agbalaka, C.C., Dandekar, A.Y., Patil, S.L., Khataniar, S., Hemsath, J.R., 2008. Coreflooding studies to evaluate the impact of salinity and wettability on oil recovery efficiency. Transp. Porous Media 76, 77–94, http://dx.doi.org/10.1007/s11242-008-9235-7.

Aladasani, A., Bai, B., 2012. Investigating low-salinity water flooding recovery mechanism(s) in carbonate reservoirs. In: Proceedings of the 2012 SPE EOR Conference at Oil and Gas West Asia, Muscat, Oman, 16–18 April, SPE 155560-PP.

Alotaibi, R.M., Azmy, R.M., Nasr-El-Din, H.A., 2010. A comprehensive EOR study using low salinity water in sandstone reservoirs. In: Proceedings of the SPE Improved Oil Recovery Symposium, Tulsa, OK, USA, 24–28 April, SPE 122976. http://dx.doi.org/10.2118/129976-MS.

Anderson, W.G., 1987. Wettability literature—part 1: rock/oil/brine interactions and the effects of core handling on wettability. J. Petrol. Technol. 38 (10), 1125–1144, http://dx.doi.org/10.2118/13932-PA.

Ashraf, A., Hadia, N.J., Torsaeter, O., 2010. Laboratory investigation of low salinity waterflooding as secondary recovery process: effect of wettability. In: Proceedings of the SPE Oil and Gas India Conference and Exhibition, Mumbai, India, 20–22 January, SPE 129012. http://dx.doi.org/10.2118/129012-MS.

Austad, T., RezaeiDoust, A., Puntervold, T.. 2010. Chemical mechanisms of low salinity water flooding in sandstone reservoirs. In: Proceedings of the SPE Improved Oil Recovery Symposium, Tulsa, OK, USA, 24–28 April, SPE 129767. http://dx.doi.org/10.2118/129767-MS.

Aziz, K., Settari, A., 1979. Petroleum Reservoir Simulation. Applied Science Publishers LTD, London.

Bernard, G. G., 1967. Effect of floodwater salinity on recovery of oil from cores containing clays. In: Proceedings of the 38th Annual California Regional Meeting, Los Angeles, CA, 26–27 October, SPE 175. http://dx.doi.org/10.2118/1725-MS.

Boussour, S., Cissokho, M., Cordier, P., Bertin, H., Hamon, G., 2009. Oil recovery by low salinity brine injection: laboratory results on outcrop and reservoir cores. In: Proceedings of the 2009 SPE Annual Technical Conference and Exhibition, New Orleans, LA, USA, 4–7 October, SPE 124277. http://dx.doi.org/10.2118/124277-MS.

BP Trading Limited, 1979. Enhanced Oil Recovery by Displacement with Saline Solutions. Gulf Publishing Company, Houston, TX, ISBN: 0-87201-263-8.

Buckley, J.S., Takamura, K., Morrow, N.R., 1989. Influence of electrical charges on the wetting properties of crude oils. SPE Reserv. Eng. 4 (3), 332–340, http://dx.doi.org/10.2118/16964-PA.

Cissokho, M., Boussour, S., Cordier, P., Bertin, H., Hamon, G., 2009. Low salinity oil recovery on clayey sandstone: experimental study. In: Proceedings of the International Symposium of the Society of Core Analysts, Noordwijk aan Zee, The Netherlands, 27–30 September, SCA2009-05.

Corey, A.T., 1954. The interrelations between gas and oil relative permeabilities. Prod. Monthly 19, 38–41.

Fairchild, I., Hendry, G., Quest, M., Tucker, M., 1988. Geochemical analysis of sedimentary rocks. In: Tucker, M.E. (Ed.), Techniques in Sedimentology. Blackwells, Oxford, pp. 274–354.

Gamage, P., Thyne, G., 2011. Comparison of oil recovery of low salinity waterflooding in secondary and tertiary recovery modes. In: Proceedings of the SPE Annual Technical Conference and Exhibition, Denver, CO, USA, 30 October–2 November 2011, SPE 147375. http://dx.doi.org/10.2118/124277-MS.

Hadia, N., Lehne, H.H., Kumar, K.G., Selboe, K., Stensen, J.A., Torsaeter, O., 2011. Laboratory investigation of low salinity waterflooding on reservoir rock samples from the Froy field. In: Proceedings of the SPE Middle East and Gas Show and Conference, Manama, Bahrain, 25–28 September, SPE 141114. http://dx.doi.org/10.2118/141114-MS.

Honarpour, M.M., McGee, K.R., Crocker, M.E., Maerefat, N.L., Sharma, B., 1986. Detailed core description of a dolomite sample from the Upper Madison Limestone Group. In: Proceedings of the SPE Rocky Mountain Regional Meeting, Billings, MT, USA, 19–21 May, SPE15174. http://dx.doi.org/10.2118/15174-MS.

Israelachvili, J.N., 1991. Intermolecular and Surface Forces, 2nd ed. Academic Press, San Diego, CA (ISBN-10: 0123751810).

Javandel, I., Doughty, C., Tsang, C.F., 1984. Groundwater Transport Handbook of Mathematical Models, American Geophysical Union. Water Resources Monograph 10, Washington, D.C.

Jerauld, G.R., Lin, C.Y., Webb, K.J., Seccombe, J.C., 2006. Modeling low-salinity waterflooding. IN: Proceedings of the SPE Annual Technical Conference and Exhibition, San Antonio, TX, 24–27 September, SPE 102239. http://dx.doi.org/10.2118/102239-MS.

Lager, A., Webb, K.J., Black, C.J.J., 2007. Impact of brine chemistry on oil recovery. In: Proceedings of the 14th European Symposium on Improved Oil Recovery, Cairo, Egypt, 22–24 April, Paper A24.

Lager, A., Webb, K.J., Black, C.J.J., Singleton, M., Sorbie, K.S., 2006. Low salinity oil recovery—an experimental investigation. In: Proceedings of the International Symposium of the Society of Core Analysts, Trondheim, Norway, 12–16 September, SCA 2006-36.

Lager, A., Webb, K.J., Black, C.J.J., Singleton, M., Sorbie, K.S., 2008b. Low salinity oil recovery—an experimental investigation. Petrophysics 49 (1), 28–35 (2008-v49n1a2).

Lager, A., Webb, K.J., Collins, I.R., Richmond, D.M., 2008a. LoSal™ enhanced oil recovery: evidence of enhanced oil recovery at the reservoir scale. In: Proceedings of the SPE/DOE Symposium on Improved Oil Recovery, Tulsa, OK, USA, 20–23 April, SPE 113976. http://dx.doi.org/10.2118/113976-MS.

Lee, S.Y., Webb, K.J., Lager, A., Clarke, S.M., O'Sullivan, A.F., Wang, X., 2010. In: Proceedings of the 2010 SPE Improved Oil Recovery Symposium, Tulsa, OK, 24–28 April, SPE 129722. http://dx.doi.org/10.2118/129722-ms.

Ligthelm, D.J., Gronsveld, J., Hofman, J.P., Brussee, N.J., Marcelis, F., Van der Linde, H. A., 2009. Novel waterflooding strategy by manipulation of injection brine composition. In: Proceedings of the SPE EUROPEC/EAGE Annual Conference and Exhibition, Amsterdam, The Netherlands, 8–11 June, SPE 119835. http://dx.doi.org/10.2118/119835-ms.

Liu, Y., Grigg, R.B., Bai. B., 2005. Salinity, pH, and surfactant concentration effects on CO_2-foam. In: Proceedings of the 2005 SPE International Symposium on Oilfield Chemistry, Houston, TX, 2–4 February, SPE 93095. http://dx.doi.org/10.2118/93095-ms.

McGuire, P.L., Chatham, J.R., Paskvan, F.K., Sommer, D.M., Carini, F.H., 2005. Low salinity oil recovery: an exciting new EOR opportunity for Alaska's North slope. In: Proceedings of the SPE Western Regional Meeting, Irvine, CA, 30 March–1 April, SPE 93903. http://dx.doi.org/10.2118/93903-ms.

Nasralla, R., Alotaibi, M. B., Nasr-El-Din, H.A., 2011a. Efficiency of oil recovery by low salinity water flooding in sandstone reservoirs. In: Proceedings of the SPE Western North American Regional Meeting, Anchorage, AK, USA, 7–11 May, SPE 144602. http://dx.doi.org/10.2118/144602-MS.

Nasralla, R., Nasr-El-Din, H.A., 2011b. Coreflood study of low salinity water injection in sandstone reservoirs. In: Proceedings of the SPE/DGS Saudi Arabia Section Technical Symposium and Exhibition, Al-Khobar, Saudi Arabia, 15–18 May, SPE 149077. http://dx.doi.org/10.2118/149077-MS.

Parker, J.C., Lenhard, R.J., Kuppusamy, T., 1987. A parametric model for constitutive properties governing multiphase flow in porous media. Water Resour. Res. 23 (4), 618–624.

Paul, G.W., Froning, H.R., 1973. Salinity effects of micellar flooding. J. Petrol. Technol. 25 (8), 957–958, http://dx.doi.org/10.2118/4419-PA.

Pu, H., Xie, X., Yin, P., Morrow, N.R., 2010. Low salinity waterflooding and mineral dissolution. In: Proceedings of the SPE Annual Technical Conference and Exhibition, Florence, Italy, 19–22 September, SPE 134042. http://dx.doi.org/10.2118/149077-MS.

Rivet, S. M., Lake, L.W., Pope, G.A., 2010. A coreflood investigation of low-salinity enhanced oil recovery. In: Proceedings of the SPE Annual Technical Conference and Exhibition, Florence, Italy, 19–22 September, SPE 134297. http://dx.doi.org/10.2118/134297-MS.

Robertson, E.P., 2010. Oil recovery increases by low-salinity flooding: Minnelusa and Green River formations. In: Proceedings of the SPE Annual Technical

Conference and Exhibition, Florence, Italy, 19–22 September, SPE 132154. http://dx.doi.org/10.2118/132154-MS.
Satter, A., Iqbal, G.M., Buchwalter, J.L., 2008. Practical Enhanced Reservoir Engineering: Assisted with Simulation Software. PennWell Corporation, Tulsa, OK, USA (ISBN-13:978-1-59370-056-0).
Seccombe, J.C., Lager, A., Webb, K., Jerauld, G., Fueg, E., 2008. Improving waterflood recovery: LoSal™ EOR field evaluation. In: Proceedings of the SPE/DOE Symposium on Improved Oil Recovery, 20–23 April 2008, Tulsa, OK, USA, 113480. http://dx.doi.org/10.2118/113480-ms.
Seccombe, J., Lager, A., Jerauld, G., Jhaveri, B., Buikema, T., Bassler, S., Denis, J., Webb, K., Cockin, A., Fueg, E., 2010. Demonstration of low-salinity EOR at interwell scale, Endicott Field, Alaska. In: Proceedings of the SPE Improved Oil Recovery Symposium, Tulsa, OK, USA, 24–28 April, SPE 129692. ISBN:978-1-55563-289.
Sharma, M.M., Filoco, P.R., 2000. Effect of brine salinity and crude-oil properties on oil recovery and residual saturations. Soc. Petrol. Eng. J. 5 (3), 293–300, http://dx.doi.org/10.2118/65402-PA.
Tang, G., Morrow, N.R., 1997. Salinity, temperature, oil composition and oil recovery by waterflooding. SPE Reserv. Eng. 12 (4), 269–276, http://dx.doi.org/10.2118/36680-PA.
Tang, G., Morrow, N.R., 1999a. Oil recovery by waterflooding and imbibition—invading brine cation valency and salinity. In: Proceedings of the International Symposium of the Society of Core Analysts, Golden, CO, August, SCA 9911.
Tang, G., Morrow, N.R., 1999b. Influence of brine composition and fines migration on crude oil/brine/rock interactions and oil recovery. J. Petrol. Sci. Eng. 24 (2), 99–111, http://dx.doi.org/10.1016/S0920-4105(99)00034-0.
Thyne, G., Gamage, P., 2011. Evaluation of the effect of low salinity waterflood for 26 fields in Wyoming. In: Proceedings of the SPE Annual Technical Conference and Exhibition, Denver, CO, USA, 30 October–2 November, SPE 147410. http://dx.doi.org/10.2118/147410-MS.
Van Genuchen, M.Th., 1980. A closed-form equation for predicting the hydraulic conductivity of unsaturated soils. Soil Sci. Soc. Am. J. 44, 892–898.
Vledder, P., Fonseca, J.C., Wells, T., Gonzalez, I., Lighelm, D., 2010. Low salinity water flooding: proof of wettability alteration on a field wide scale. In: Proceedings of the SPE Improved Oil Recovery Symposium, Tulsa, OK, USA, 24–28 April, SPE 129692. http://dx.doi.org/10.2118/129564-ms.
Yousef, A.A., Al-Saleh, S., Al-kaabi, A., Al-Jawfi, M., 2010. Laboratory investigation of novel oil recovery method for carbonate reservoirs. In: Proceedings of the Canadian Unconventional Reservoirs & International Petroleum Conference, Calgary, Alberta, Canada, 19–21 October, CSUG/SPE 137634. http://dx.doi.org/10.2118/137634-PA.
Yildiz, H.O., Valat, M., Morrow, N.R., 1999. Effect of brine composition on wettability and oil recovery of a Prudhoe Bay crude oil. J. Can. Petrol. Technol. 38 (1), 26–31.
Webb, K.J., Black, C.J.J., Al-Ajeel, H., 2004. Low salinity oil recovery—log-inject-log. In: Proceedings of the SPE/DOE Symposium on Improved Oil Recovery, Tulsa OK, 17–21 April, SPE 89379-MS. http://dx.doi.org/10.2118/89379-ms.
Wu, Y.S., Forsyth, P.A., Jiang, H., 1996. A consistent approach for applying numerical boundary conditions for multiphase subsurface flow. J. Contam. Hydrol. 23, 157–184.
Wu, Y., Bai, B., 2009. Efficient simulation of low-salinity waterflooding in porous and fractured reservoirs. In: Proceedings of the 2009 SPE Reservoir Simulation Symposium, The Woodlands, TX, 2–4 February, SPE 118830. http://dx.doi.org/10.2118/118830-ms.
Zhang, Y., Morrow, N.R., 2006. Comparison of secondary and tertiary recovery with change in injection brine composition for crude oil/sandstone combinations. In: Proceedings of the 2006 SPE/DOE Symposium on Improved Oil Recovery, Tulsa, OK, USA, 22–26 April, SPE 99757. http://dx.doi.org/10.2118/99757-MS.
Zhang, Y., Xie, X., Morrow, N. R., 2007. Waterflood performance by injection of brine with different salinity for reservoir cores. In: Proceedings of the SPE Annual Technical Conference and Exhibition, Anaheim, CA, USA, 11–14 November, SPE 109849. http://dx.doi.org/10.2118/109849-ms.